PARAMETERS OF CREEP CRACK GROWTH - CLASSIFICATION AND LIMITS

R. Kienzler* and T. Hollstein†

Experimental, numerical and theoretical results describing the creep crack growth behaviour of several high temperature steels and alloys are reported. The alloys chosen cover a wide range of deformation behaviour and of crack tip controlling parameters like stress-intensity factor K, C^*-integral, C_h^* -integral, and J-integral. The results are discussed in terms of a load-parameter map.

INTRODUCTION

The assessment of cracks in creeping materials is an essential matter. For ferritic steels above some 400°C, e.g., deformation and fracture become time-dependent and components operating in such a creep regime may fail by growth of possible pre-existing flaws even at low load levels. Due to stress concentrations in real structures, diffusion processes and cavity nucleation and growth are highly localized such that macroscopic cracks develop. Fracture-mechanics concepts are expected to describe the failure of such components.

The general idea of these concepts is that the crack-tip stress and strain fields are characterized - under certain limiting conditions - by a single parameter independently on the size and geometry of the structure or the loading condition. If the parameter is identified, creep crack growth should be correlated with it. Whether those concepts really decribe crack initiation and crack growth, must be determined, of course, experimentally.

* Universität Bremen, Fachbereich Produktionstechnik, D-28334 Bremen
† Fraunhofer-Institut für Werkstoffmechanik, D-79108 Freiburg

The aim of the paper is to summerize results in a more general setting, that have been obtained experimentally and numerically during recent years. To this end the findings are fitted into a load-parameter map according to Riedel (1).

Details of the experimental and numerical prodedure, chemical composition and heat treatment of materials, etc. may be found in (2) and in the literature cited subsequently.

CREEP FRACTURE PARAMETERS; CHARACTERISTIC TIMES

In analogy to Hutchinson, Rice and Rosengren (HRR), Riedel and Rice (3) developed the near-crack-tip fields for power-law-creep materials. Let r and φ be polar coordinates with origin at the crack tip, stresses and strains are given by

$$\sigma_{ij} = \sigma_0 \left(\frac{C(t)}{A\ \sigma_0\ \dot{\varepsilon}_0\ I_n\ r} \right)^{1/(n+1)} \tilde{\sigma}_{ij}(\varphi,n), \qquad \text{.....(1)}$$

$$\dot{\varepsilon}_{ij} = A\ \dot{\varepsilon}_0 \left(\frac{C(t)}{A\ \sigma_0\ \dot{\varepsilon}_0\ I_n\ r} \right)^{n/(n+1)} \tilde{\dot{\varepsilon}}_{ij}(\varphi,n). \qquad \text{.....(2)}$$

A, n, $\dot{\varepsilon}_0$, σ_0. are the constants of Norton's creep law

$$\dot{\varepsilon} = A\ \dot{\varepsilon}_0 \left[\frac{\sigma}{\sigma_0} \right]^n + \frac{\dot{\sigma}}{E}, \qquad \text{.....(3)}$$

whereas the constant I_n and the dimensionless functions $\tilde{\sigma}_{ij}$ and $\tilde{\dot{\varepsilon}}_{ij}$ are tabulated by Hutchinson (4).

Immediately after loading the instantaneous response of the specimen is - depending on the load level - purely elastic or elastic plastic. Riedel and Rice showed that the time-dependent loading parameter C(t) for this short time domain is calculated by

$$C(t) = \frac{J}{(n+1)t} \qquad \text{.....(4)}$$

with J being Rice's J-integral (5), the dominant parameter of elastic-plasic fracture mechanics. If the material behaves mostly elastic, Irwin's relation is applicable relating J to the stress-intensity factor K by

$$K^2 = J/E'. \qquad \text{.....(5)}$$

(E' = E for plane stress, E' = $E/(1-\nu^2)$ for plane strain, Young's modulus E, Poisson's ratio ν).

For the long-time regime, the C^*-integral (3) becomes the characteristic parameter of the near-tip fields

$$C(t) = C^*. \qquad \text{.....(6)}$$

The characteristic time indicating the transition from small-scale creep (short-time regime) to steady-state creep (long-time regime) is estimated by (3)

$$t_1 = \frac{J}{(n+1)C^*}. \qquad \text{.....(7)}$$

The transition time t_1 depends on load level, material and temperature and might be of the order of minutes up to years (6).

In a similar manner, the parameter of primary creep C_h^* and a respective transition time t_2 between primary and secondary creep might be introduced (6).

The regimes in which different load parameters are valid can be represented conveniently on a load-parameter map (Figure 1). This is a diagram with the logarithm of time versus the logarithm of a load measure, e.g., reference stress (1). For low load levels an area of predominant diffusion creep is included. The diagram is bounded by the time to fracture t_f and by the limitation to C^* due to crack-tip blunting t_b. The illustration is, of course, schematic. The results of previous creep crack growth investigations of the authors are drawn into this time-stress plane.

INVESTIGATION OF SEVERAL HIGH-TEMPERATURE ALLOYS

The "creep ductile" alloy Ni Cr 22 Co 12 Mo (IN 617) has been tested (7) in loading ranges where crack growth in compact specimens is C^*-controlled (region 1 in Figure 1) and where crack growth in tension specimens with through and part-through cracks is characterized by limit load behaviour due to large crack-tip deformations and the corresponding low intensity of the crack-tip

stress state (region 2). The corresponding creep-crack-growth rate vs. C^*-curves are shown in Figure 2, where only crack-growth rates of the CT-specimens are correlated with C^*. Crack-growth rates of the tensile specimens, however, seem to be independent of C^*.

Alloy 800 H has been investigated (8) in the transition region of C^*-to J-controlled crack growth (Figure 3). Under C^*-controlled conditions the experimental data of crack growth are described for a wide range of geometries of flaws and specimens by a power law (region 6, Figure 1)). For higher loadings with increasing plastic deformations, crack growth is J-controlled (region 7).

The more "creep brittle" alloy NIMONIC 80 A has been tested (9) in a load range with K-controlled creep crack growth for short times after loading and for low loads (see region 3 in Figure 1). In Figure 4 crack-growth rate and values of the stress intensity factor K at attainment of a constant crack-opening-displacement rate are plotted. In this load range elastic effects are dominating. For longer times above the transition time t_1 of typically 200 hours, crack growth is C^*-controlled (see region 4 in Figure 1 and Figure 5). For high loads above the yield strengh, plastic effects are dominating, and the crack-growth behaviour is J-controlled (region 5).

The steel 21 Cr Mo Ni V 5 7 (1 % Cr-steel) at 550° (10, 11) behaves similar to NIMONIC 80 A at 650°C. For short times and low loadings linear elastic effects are dominant, and crack growth can be described with the stress intensity factor K by a power law, independent of the geometry of flaw and specimen (see Figure 6 and Figure 1, region 8). For times above the transition time t_1 crack growth is C^*-controlled as shown in region 9 of Figure 1 and in Figure 7. A comparison to a model of Nikbin et al. (12) shows in addition that the creep-crack-growth rates can be described assuming plane-stress conditions, which has been found also experimentally for other materials (11, 12) and numerically on the basis of FE-calculations for several specimens from materials discussed in this paper (2). The deviation of the 12-hour test and of one CN-specimen test from the otherwise narrow scatterband in Figure 7 can be explained by an increase of plastic deformation and a loss of constraint, respectively, which result in lower crack-growth rates.

9 - 12 % Cr-steels show K-controlled crack growth for appropriate loadings (region 10). This is documented in Figure 8 with experimental results from three different papers (13-15) with CT-specimens taken from X20 Cr Mo V 12 1 at 550° C. If a description of the crack-growth behaviour is tried using C^*, all data are indeed in one common but large scatterband, the data of the individual tests, however, cannot be described by a common power law (8).

For the stainless steel X 6 Cr Ni 18 11 (A 304), creep crack growth under primary creep conditions has been realized (region 11). Here creep crack growth is described by C_h^* (16). For stationary creep conditions, again C^* describes the crack growth behaviour in a geometry-independent manner.

CONCLUDING REMARKS

The discussion of creep-crack growth of different high-temperature materials in terms of a load-parameter map exhibits possibilities and limits of a fracture-mechanics description. For the investigation performed so far, regions exist - as shown in Figure 1 - where fracture-mechanics parameters K, J, C^*, and C_h^* characterize the stress singularity at a crack tip and control crack-growth behaviour. For the transition between one region of the load-parameter map to another is estimated asymptotically, the passages occur gradually. If specimens or components are operated in a transition regime, interpolation formulae are to be used that are provided in the literature, e.g., (1), (17) and (18).

As shown in Figures 2, 3, 5 and 7 creep-crack growth under steady-state creep conditions and the corresponding crack-tip parameter C^* are correlated by a power law $\dot{a} \sim (C^*)^{\alpha}$. The exponent α coincides almost perfectly with the theoretical value of n/(n+1) that Riedel (6) deduced by use of a micro-void model. Limits of the power-law correlation due to extended crack-tip blunting and to loss of constraint by inadmissible plastic deformations have been exceeded with CN-specimens from Ni Cr 20 Co 12 Mo material (region 2, Figure 1) and with a highly-loaded DEN-specimen from Nimonic 80 A (region 5, Figure 1), respectively.

The short-time behaviour of NIMONIC 80 A, 21 Cr Mo Ni V 5 7 and X 20 Cr Mo V 12 1 is dominated by the stress intensity factor K (region 3,8,10 of Figure 1 and Figures 4, 6 and 8, respectively). As indicated in the Figures, again, a power-law correlation $\dot{a} \sim (K)^{\beta}$ seems to exist with an exponent β ranging between about 2 and 10. Theoretical models for the theoretical prediction of β ar not at hand presently.

REFERENCES

(1) Riedel, H., "Creep Crack Growth", ASTM-STP 1020, American Society for Testing and Materials, 1989, pp. 191-126.
(2) Kienzler, R., "Konzepte der Bruchmechanik", Vieweg, 1993.
(3) Riedel, H., and Rice, J. R., " Tensile Cracks in Creeping Solids", ASTM-STP 700, American Society for Testing and Materials, 1980, pp. 112-130.
(4) Hutchinson, J. W., J. Mech. Phys. Solids, Vol 16, 1968, pp. 337-347.
(5) Rice, J. R., J. Appl. Mech, Vol. 35, 1968, pp. 379-386.

(6) Riedel, H., "Fracture at High Temperatures", Springer, 1987.

(7) Kienzler, R. and Hollstein, T., "Experimental and Numerical Investigation of Creep Crack Growth", Proceedings of the Third International Conference on Creep and Fracture of Engineering Materials and Structures, Edited by B. Wilshire and R. W. Evans, Swansea, U. K., 1987, pp. 563-576.

(8) Hollstein, T. and Kienzler, R., J. Strain Analysis, Vol 23, 1988, pp. 87-96.

(9) Hollstein, T. and Kienzler, R., "Numerische und experimentelle Untersuchungen zum Kriechrißwachstum. IWM-Report W1/91, Fraunhofer-Institut für Werkstoffmechanik, Freiburg, Germany, 1991.

(10) Hollstein, T. and Kienzler, R., "Investigation of Creep Crack Growth: A Comparison between Experimental and Numerical Results", Proceedings of MECAMAT "High Temperature Mechanisms and Mechanics", EGF6, Edited by P. Bensussan and J. P. Mascarell, Mechanical Engineering Publications, London, 1990, pp. 339-351.

(11) Hollstein, T. et al., Materials at High Temperature, Vol 10, 1992, pp. 92-96.

(12) Nikbin, K. M. et al., ASME J. Eng. Mater. Technol., Vol 108, 1986, pp. 186-191.

(13) Mohrmann, R., Sester, M. and Hollstein, T., "Application of a micro-mechanical material model on creep damage and on creep crack growth in X20 Cr Mo V 12 1 ", this conference proceedings.

(14) Hollstein, T. and Gnirß, G., "Ermittlung von Kriech- und Ermüdungsrißwachstum in X20 Cr Mo V 12 1 zur Bauteilbewertung", Tagungsband der 17. Sitzung des Arbeitskreises Bruchvorgänge im DVM, Basel, 1985, pp. 79-100.

(15) Speidel, M., unpublished results, 1982.

(16) Hollstein, T. and Kienzler, R., Mat.-wiss. u. Werkstofftech., Vol 20, 1989, pp. 396-404.

(17) Saxena, A., "Creep Crack Growth under Non-Steady State Conditions", ASTM-STP 905, American Society for Testing and Materials, 1986, pp. 185-201.

(18) Ainsworth, R. A. et al., Fatigue Fract. Engng. Mater. Struct., Vol. 10, 1987, pp 115-127.

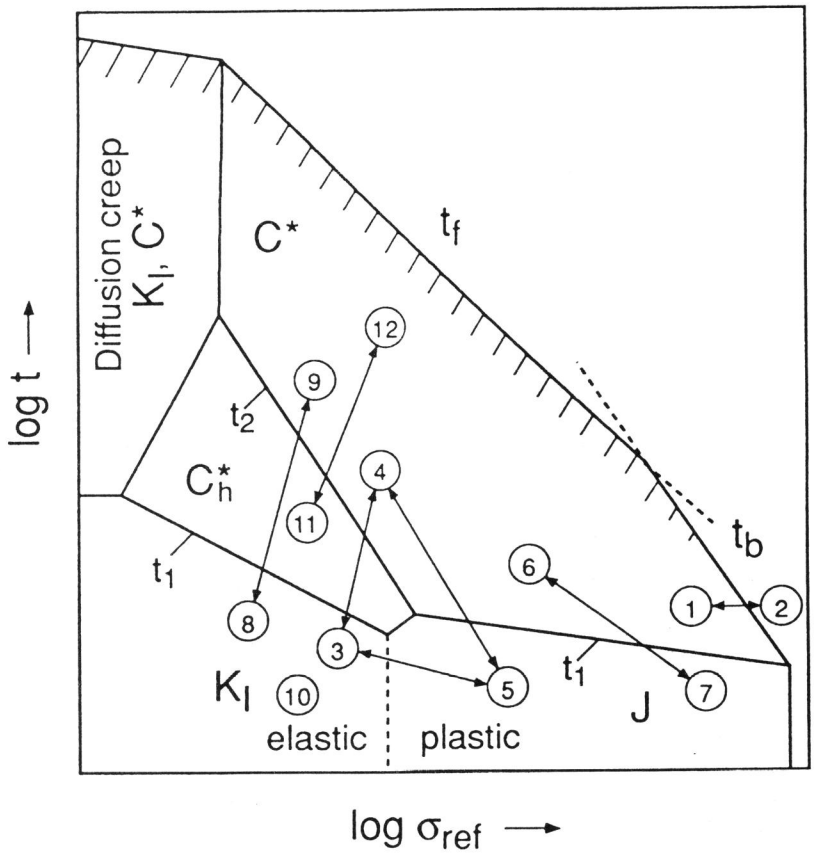

Legend

INCOLOY 800 H:
6: low load, long time
7: high load, short time

Ni Cr 22 Co 12 Mo:
1: CT-specimen
2: CN-, PTC-specimen

21 Cr Mo Ni V 57
8: short time 9: long time

NIMONIC 80 A:
3: CT-, SEN-specimen, short time
4: CT-, SEN-specimen, long time
5: DEN-specimen

10: 9-12 % Cr-steels

X 6 Cr Ni 18 11
11: short time 12: long time

Figure 1 Load-parameter map (schematic); regimes of dominant crack-tip loading parameters

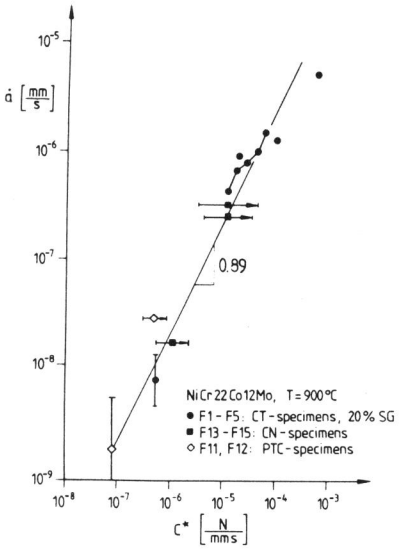

Figure 2: á vs. C* for NiCr22Co12Mo at 900°C

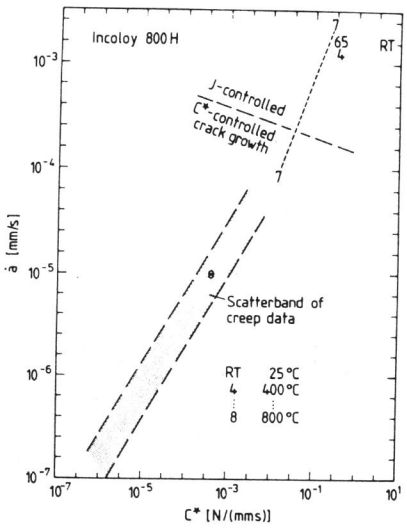

Figure 3: á vs. C* for Incoloy 800H from RT to 800°C

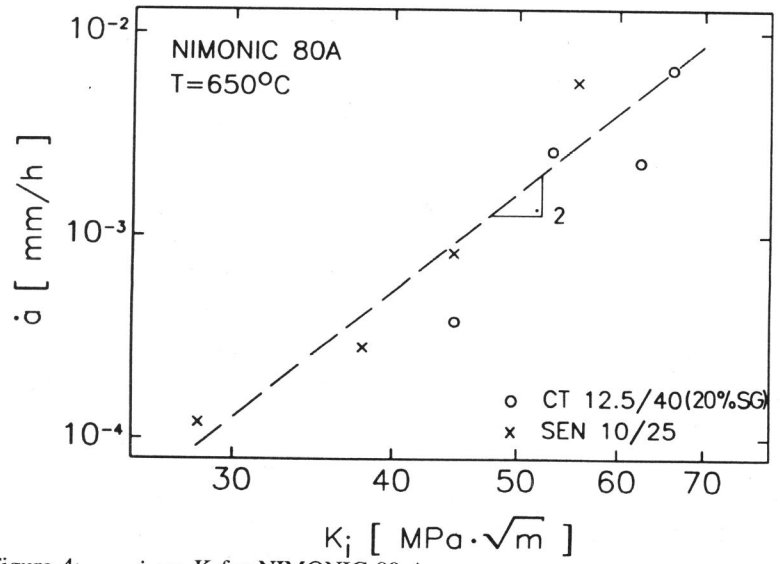

Figure 4: á vs. K for NIMONIC 80 A, short time after loading

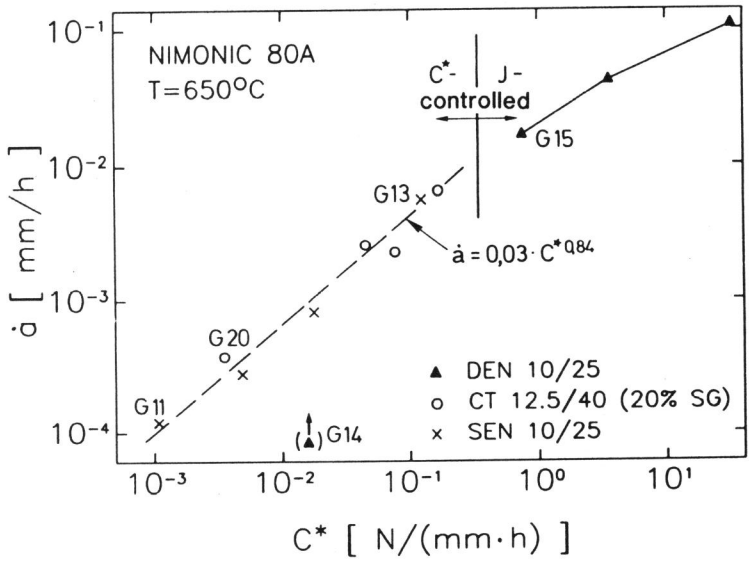

Figure 5: ȧ vs. C* for NIMONIC 80 A, long-time regime

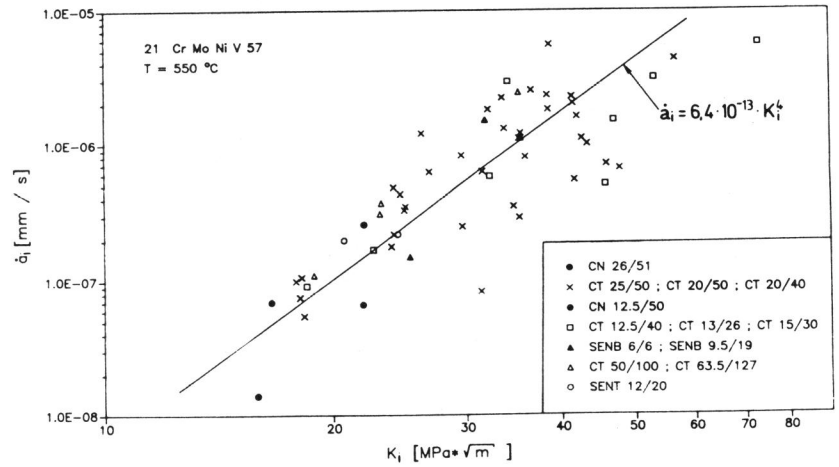

Figure 6: ȧ vs. K for 21 Cr Mo Ni V 5 7 at 550°C, short time

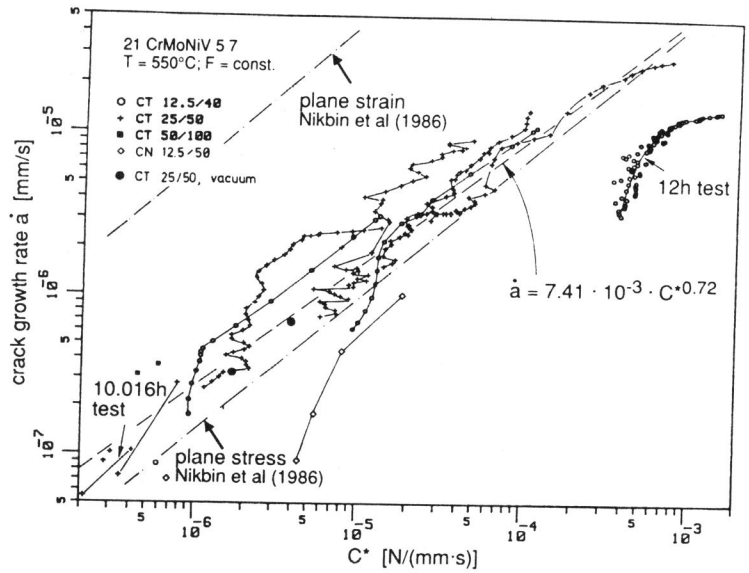

Figure 7: ȧ vs. C* for 21 Cr Mo Ni V 5 7 at 550°C, long time

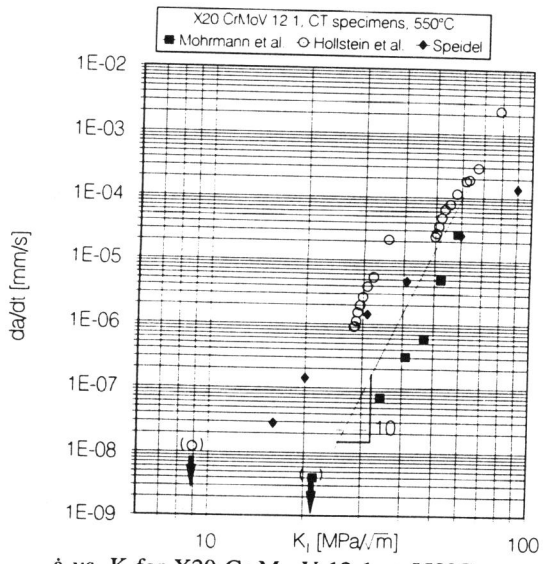

Figure 8: ȧ vs. K for X20 Cr Mo V 12 1 at 550°C; ref.: Mohrmann et al. (13), Hollstein et al. (14), Speidel (15)